inter.noise
HAMBURG 2016

Impedance deduction for vegetated roof surfaces: multiple geometry strategy

Chang LIU[1]; Maarten HORNIKX[1]

[1] Eindhoven University of Technology, The Netherlands

ABSTRACT

The transfer function method is an efficient procedure to deduce the ground surface impedance from short-range propagation measurements using one point source. It is able to provide a reasonable prediction of the surface impedance of a vegetated roof as well, and the characteristics of the vegetated roof can be explored by fitting an impedance model to the deducted surface impedance thereafter. However, the surface impedance is sensitive to the adopted measurement locations of transducers, and the impedance fitting procedure is dependent on the starting values of the impedance model parameters. This work shows the sensitivity of the predicted surface impedance on the adopted transducers' locations. In addition, the uniqueness of the fitting procedure will be investigated by multiple geometry setups on porous materials in a laboratory condition. This multiple setups practice and an improved measurement system can be employed to deduce the surface impedance of in-situ vegetated roof systems.

Keywords: Vegetated roof, surface impedance deduction I-INCE Classification of Subjects Number(s): 55

1. INTRODUCTION

The normalized ground surface impedance is an important acoustic property to predict outdoor sound propagation (1). It can be determined by the prediction from an impedance model or by the deduction from an in-situ measurement (2). Nocke and Mellert (3), Taherzadeh and Attenborough (4), and Dutilleux *et al.* (5) have explored the transfer function method to deduce the impedance of a ground surface in-situ. However, few studies focused on the prediction of the impedance of vegetated roofs with its low flow resistivity (6, 7).

The acoustic impedance and properties of vegetated roofs were investigated using a short range propagation method by fitting level differences between two receivers based on the Nordtest method (8). However, it was found that no unique acoustic parameters could be obtained by this technique. Hess *et al.* (9) and Taherzadeh and Attenborough (4) proposed a multiple-geometry technique to avoid non-unique values, which means that three configurations are required to deduce three variables. However, the approach to predict the surface impedance with multiple geometries has not been verified for vegetated roofs.

The multiple-geometry technique was verified on vegetated roofs by level differences fitting using the slit pore impedance model. The geometries taken in the experiments were similar to that in the Nordtest method (10). As shown in Figure 1 and Figure 2, the predicted acoustic impedance can be physically reasonable, but the predicted sound pressure level differences at the interference peaks differ from the measured sound pressure level differences. As the sound pressure caused by a single sound source above the ground surface is characterized by the interference of the direct and ground reflected sound waves (3, 11), the accuracy in determining the location of the transducers influences the prediction of ground surface impedance. Thus, an error in the deduction of the path length of direct and indirect waves can be responsible for this impact. Indeed, Kruse and Mellert identified that the quality of the performance of the ground impedance prediction can be degraded by an inaccurate measurement of the distance between source and receivers (12). However, further research still is needed on the evaluation of the influence of the adopted transducers' locations.

This paper starts with a brief introduction about the experimental procedure to extract the surface impedance using the transfer function method. Thereafter, the accuracy of the adopted transducers'

[1] c.liu@bwk.tue.nl

locations on the predicted normalized surface impedance is analyzed. Finally, the uniqueness of the predicted acoustic parameters using a multiple setup technique is studied.

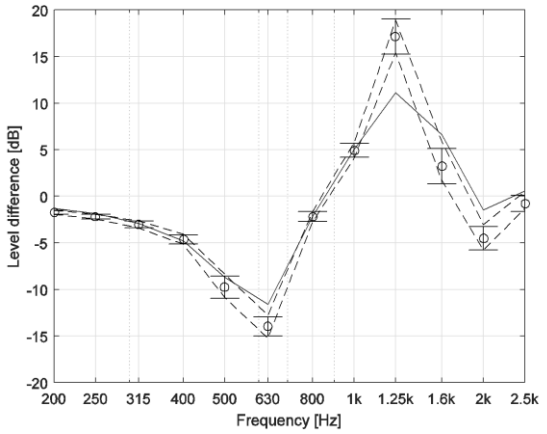

Figure 1 – The measured (circles) and predicted (solied) level differences between two receiver positions on a vegetated roof. Predicted results are obtained from a best fit of multiple setups.

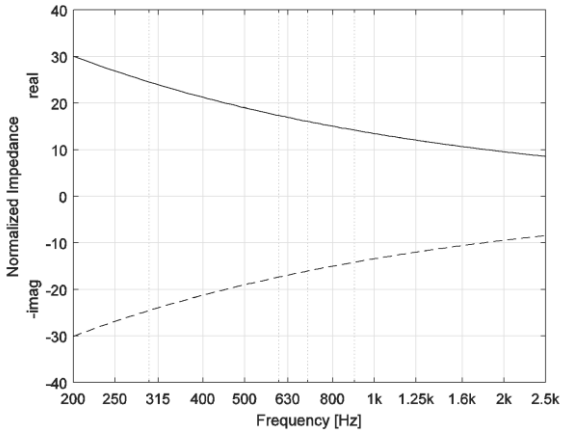

Figure 2 – The predicted impedance from the impedance model used in Figure 1.

2. EXPERIMENTAL PROCEDURE

2.1 Measurement Setup

To evaluate the measurement system, measurements were done on polyester wool (Caruso Iso Bond) in laboratory conditions. The temperature was 18.7 ºC and recordings were far above the background noise level. The main equipment used in this research consist of a broadband speaker (Visaton - FR 8 WP 8 Ohm), one omni-directional microphone (Behringer – Type: ECM8000) and one sound card with sample frequency of 192 kHz (E-MU – 0202 USB2.0). The internal MLS sound from the DIRAC 6.0 software (Bruël & Kjær /Acoustics Engineering) was emitted as the signal with a length of 5.46 s for each measurement. The recorded impulse responses were obtained using DIRAC 6.0 and analyzed in Matlab R2015b.

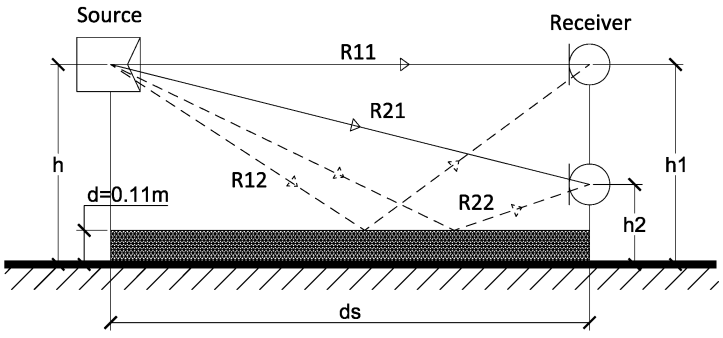

Figure 3 – Measurement Setup

Figure 4 – Measurement Setup in Laboratory

The measurement setup is shown in Figure 3 and Figure 4. The microphone was first placed on the upper position and then on the lower position to reduce the influence of microphone errors on the measurement results (13). To investigate the application of the multiple setup strategy on the uniqueness of the fitting procedure of the impedance model parameters, three geometry setups were taken. For each setup, five measurements were carried out at the same location. In order to achieve the exact locations of the transducers, pre-measurements on a hard ground surface were carried out and locations were derived from time differences of direct and reflected waves fields in the impulse responses. The geometries of three setups are presented in Table 1.

Table 1 – Geometries of three setups with extracted distances.

	Height of Source (h_s) [m]	Height of upper receiver (h_{r1}) [m]	Height of lower receiver (h_{r2}) [m]	Horizontal distance between source and receivers (d_{sr}) [m]
Setup 1	0.506	0.50	0.20	1.792
Setup 2	0.802	0.80	0.20	1.157
Setup 3	0.602	0.60	0.35	1.782

2.2 Deduction of Surface Impedance

The direct deduction of the ground surface impedance is based on the short-range propagation measurements using one point source and two receiver positions from Section 2.1. From the measurement results, the sound pressure as a function of frequency at each receiver position can be achieved. This ratio of the sound pressure of two microphones is defined as the complex transfer function (T_{meas}) in Equation (1).

$$T_{meas} = P_{1,meas} / P_{2,meas} . \tag{1}$$

On the other hand, the frequency dependent transfer function (T_{pred}) as shown in Equation (2) can be calculated with two unknown variables - the real and imaginary part of the surface impedance (Z_d) – and a set of known variables: the angle of incident sound waves with the ground surface, the direct path lengths between source and receivers and ground reflected path lengths between source and receivers (3, 4). Here, the surface of the porous material is supposed to be a locally reacting surface because non locally reacting surfaces require specification of four parameters which cannot be determined uniquely (3).

$$T_{pred} = P_{1,pred} / P_{2,pred} . \tag{2}$$

Then, the surface impedance (Z_d) per frequency can be deducted by finding the best fit of the predicted transfer function to the measured transfer function per frequency. The fitting error (E1) is defined as:

$$E1 = \left|real(T_{pred} - T_{meas})\right|^2 + \left|imag(T_{pred} - T_{meas})\right|^2 . \tag{3}$$

2.3 Deduction of Acoustic Impedance Model Parameters

The acoustic impedance model parameters of porous materials are explored by fitting the impedance (Z_m) to the impedance (Z_d) as derived in Section 2.2 in the frequency range from 200 Hz to 2500 Hz. The fitting error (E2) is defined as:

$$E2 = \sum\nolimits_f \left(\left|real(Z_m - Z_d)\right| + \left|imag(Z_m - Z_d)\right|\right) . \tag{4}$$

As impedance model in this research, the locally reacting one-layer hard backing slit-pore model is used (14), with the flow resistivity (σ), porosity (Ω), and thickness (d) of the porous material as variables.

In case of a multiple geometry strategy, the fitting error is defined as the sum of the fitting errors of the surface impedance for the three setups, with the three parameters of the acoustic impedance as

variables.

3. SENSITIVITY OF DEDUCTED IMPEDANCE ON ADOPTED TRANSDUCERS' LOCATIONS

The sensitivity of the adopted transducers' locations on the predicted impedance is studied with the variation of the height of the source (h_s), the height of the receiver (h_{r1},h_{r2}) and the horizontal distance between source and receivers (d_{sr}). The variables are increased with respect to the correct values, with an increment of ±0.005m in the range from -0.03m to 0.03m and an increment of ±0.01m in the range from -0.1m to -0.04m and from 0.04m to 0.1m.

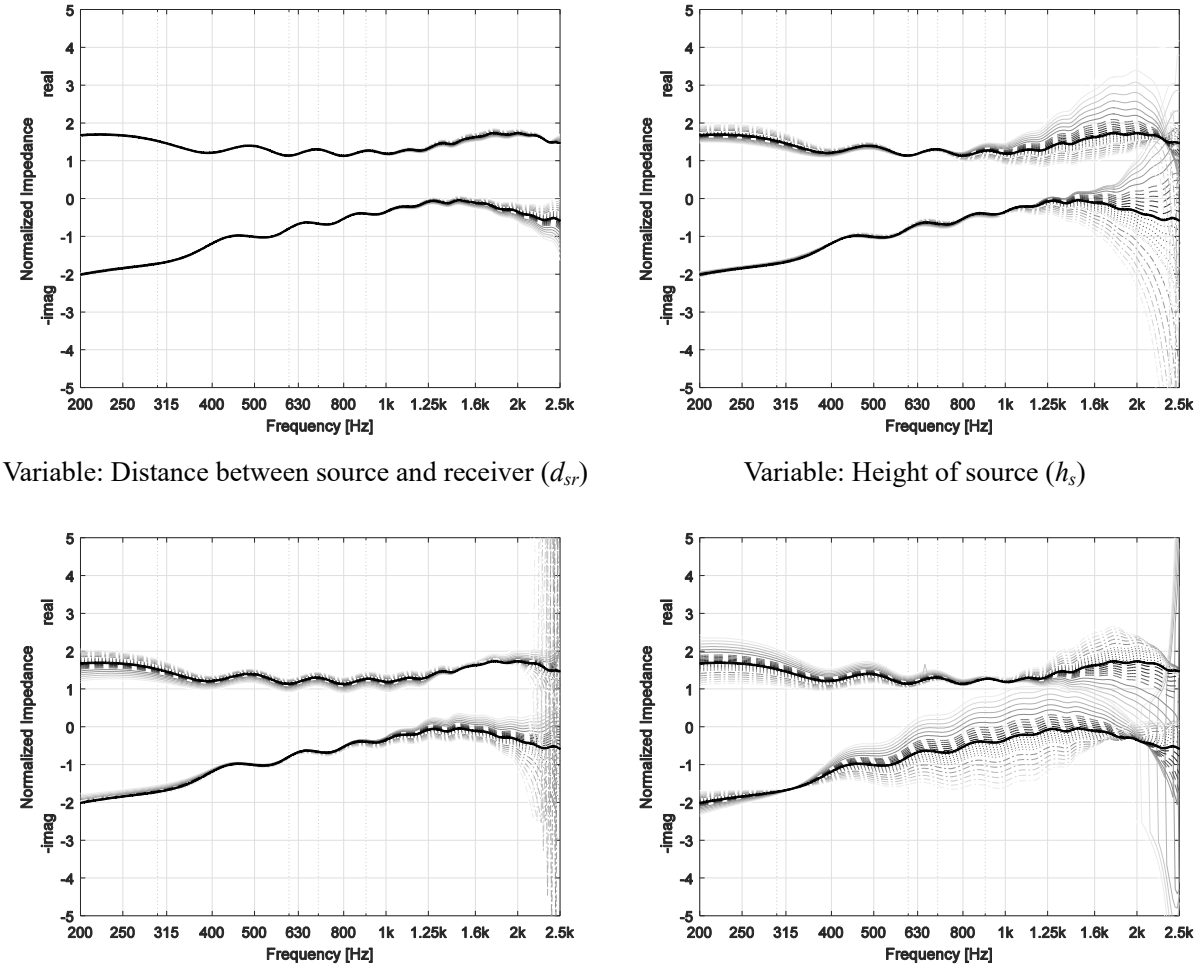

Variable: Distance between source and receiver (d_{sr})

Variable: Height of source (h_s)

Variable: Height of upper receiver (h_{r1})

Variable: Height of lower receiver (h_{r2})

Figure 5 – The predicted normalized surface impedance with the variation in variables d_{sr}, h_s, h_{r1} and h_{r2} (for Setup 1 of Table 1). (Solid thick) predicted impedance with the data from Table 1; (Solid) 7 intervals with decreasing variable deviation with increment of 0.01 m from -0,04 m down to -0,1 m; (Dashed) 7 intervals with decreasing variable deviation with increment of 0.005 m from 0 down to -0.03 m; (Dotted) 7 intervals with increasing variable deviation with increment of 0.005 m from 0m up to 0.03 m; (Dotted-dashed) 7 intervals with increasing variable deviation value with increment of 0.01 m from 0.04 m up to 0.10 m.

For setup 1 and procedure according to Section 2.2, Figure 5 shows the predicted normalized surface impedance with the variation of d_{sr}, h_s, h_{r1} and h_{r2}. A variation in the distance between source and receivers d_{sr} does only slightly influence the highest frequencies. It is clear that decreasing the height of source leads to an obvious deviation in the predicted impedance even for small increments, especially for frequencies above 1 kHz. The effect when increasing the height of source is limited on the real part of the impedance but more pronounced on the imaginary part of the impedance above 1 kHz. The height of top receiver can lead to deviations in the predicted impedance mostly above 1.6 kHz. The most outstanding influence on the deduced impedance can be found by the variation of the

height of the lower receiver, which appears at the middle frequencies between 500 Hz and 1. 6kHz on the imaginary part and frequencies below 500 Hz and above 1.25 kHz on the real part. The possible reason for this trend is that the relative phase difference between direct and ground reflected waves is largest for an offset in the location of the lower receiver.

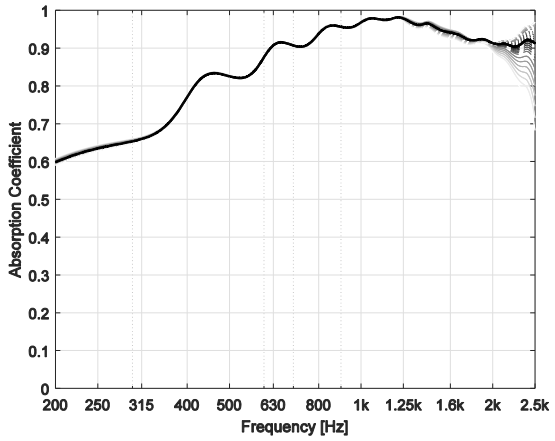

Variable: Distance between source and receiver (d_{sr})

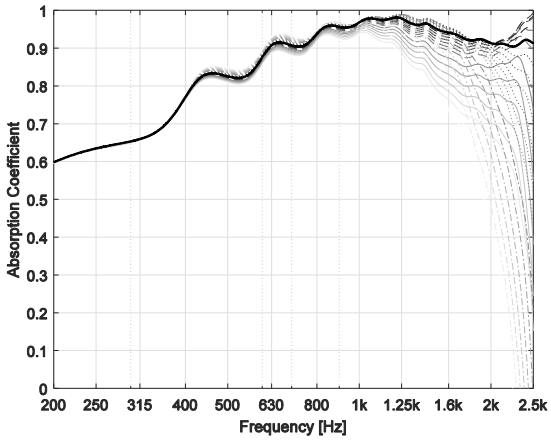

Variable: Height of source (h_s)

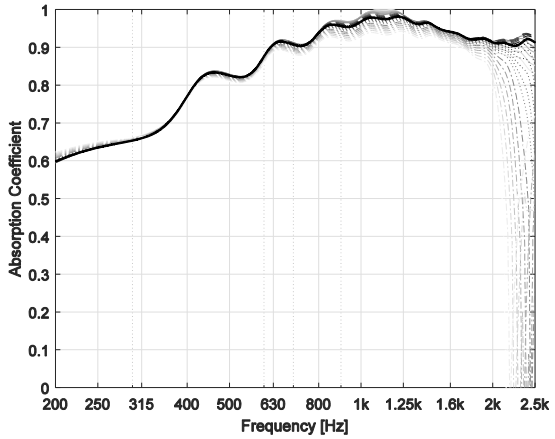

Variable: Height of upper receiver (h_{r1})

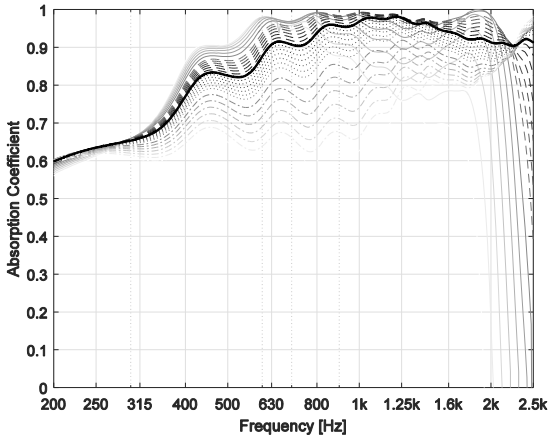

Variable: Height of lower receiver (h_{r2})

Figure 6 – As Figure 5, but for the normal incidence absorption coefficient.

Similar results can be obtained for the predicted normal incidence absorption coefficient as presented in Figure 6. The most noteworthy influence can be found with the variation of the height of the lowest receiver, where the absorption coefficient drops for most frequencies when adopting a higher value of the height and goes up when taking a lower value of the height. There is also an obvious but more limited trend of a decreasing absorption coefficient with an adopted increasing height of the source and upper receiver, especially at frequencies above 800 Hz. Only small changes can be detected with the variation of the horizontal distance between source and receivers.

4. Dependency of Fitting on Starting Values

Figure 7 and Figure 8 show the normal incidence absorption coefficient and surface impedance of the porous material fitting with three setups according to Section 2.3. The starting values of the impedance fitting procedure are 5000 kPa s /m^2 for the flow resistivity, 0.8 for the porosity and 0.11 m for the thickness, which are based on the best estimation from previous research and measurements. In general, the extracted normalized absorption coefficient of this porous material levels at around 0.95 in the frequency range between 500 Hz and 2500 Hz which can compare with the results of measuring a sample of the same material in the impedance tube. However, the dip around 1.6Hz in impedance tube results is not retrieved from the two microphone technique of Figure 3. Figure 8 shows the normalized surface impedances as deduced for the three setups according to Section 2.2. The three

curves show some dissimilarities, in particular setup 2 leads to deviating results above 1 kHz for some distinct frequencies. One of the possible reasons for that is the fact that the porous material cannot be assumed as a locally reacting surface. The thick lines in Figure 8 show the fitted impedance of the slit pore model according to Section 2.3.

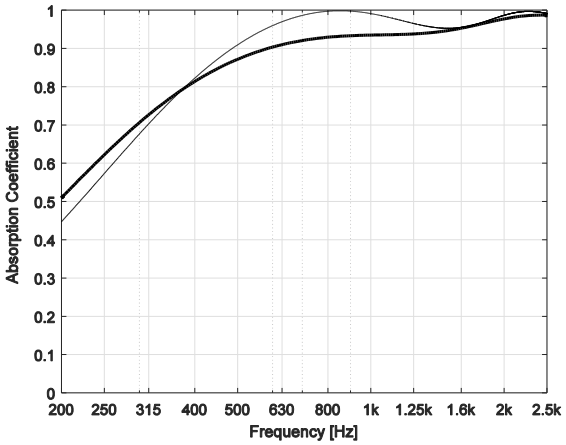

Figure 7 – The normal incidence absorption coefficient of polyester wool as deduced from different methods. (Solid thick) Multiple setup strategy using slit pore impedance model; (Solid thin) Fitted slit pore impedance model from impedance tube measurements.

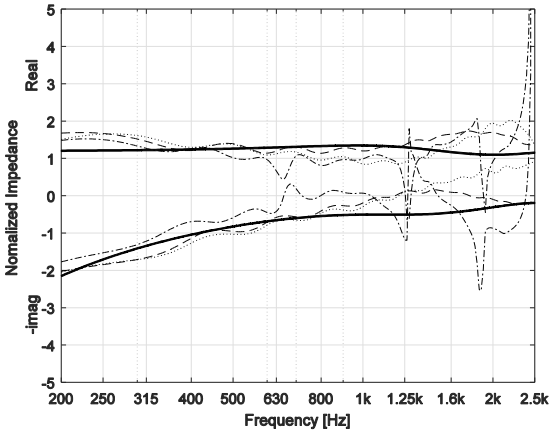

Figure 8 – The normalized surface impedance of polyester wool with the multiple setup strategy. Extracted impedance Z_d of three setups (setup 1: …; setup 2: -.-; setup 3: --) and the thick solid lines are the predicted impedance Z_m.

The predicted acoustic properties of polyester wool using three setups strategy can be found in and Table 2 with a variation of initial estimations of flow resistivity of [100-5•10^{10} kPa s /m^2], porosity of [0.1-0.9], and thickness of [0.06-0.19 m]. It can be found in Table 2 that the variation of the predicted values is less than 0.3% for all the combinations, implying that the fitting procedure is not dependent on the starting values with the multiple geometry strategy.

Table 2 – Predicted acoustic property values with the variation of initial estimations in case of three setups. Bold printed numbers indicate a change in the initial values

	Flow resistivity [kPa s m^{-2}]	Porosity [-]	Thickness [m]	Total Error E2 [kPa s m^{-2}]
Initial	**5000**	**0,80**	**0,11**	
Predicted	14616	0,93	0,10	659,56
Initial	**5E10**	0,80	0,11	
Predicted	14627	0,93	0,10	659,56
Initial	**100**	0,80	0,11	
Predicted	14627	0,93	0,10	659,56
Initial	5000	**0,10**	0,11	
Predicted	14612	0,93	0,10	659,56
Initial	5000	**0,90**	0,11	
Predicted	14628	0,93	0,10	659,56
Initial	5000	0,80	**0,06**	
Predicted	14597	0,94	0,10	659,56
Initial	5000	0,80	**0,19**	
Predicted	14636	0,93	0,10	659,56

5. CONCLUSIONS

This paper reports on preliminary studies of a method to extract the surface impedance of a vegetated roof.

For this reason, the impact of the adopted transducers' locations on the deduction of the ground surface impedance are analyzed in this research. It is found that the height of source and receivers have a significant influence on the prediction of the impedance and absorption for small errors in the adopted transducers' locations. Therefore, the accuracy of the transducers' location should be limited when deducing the ground surface impedance using transfer function method. Further research should be done on the sensitivity of the adopted transducers' locations using the Nordtest method by fitting level differences and also on the impedance prediction of other surfaces as vegetated roofs.

Also, a multiple geometry technique (three setups for three parameters to be fit in this case) is explored to obtain a unique impedance deduction of polyester wool in laboratory conditions. However, the assumption of a locally reacting surface of the material can be responsible for the dissimilarities of the predicted impedance among three setups. Thus, a further study will be carried out on the comparison of the results from a locally and non-locally assumption. Afterwards, the application of this technique on in-situ experiments of vegetated roofs will be taken.

ACKNOWLEDGEMENTS

This project has been funded by the Chinese Scholarship Council (CSC). The author would like to thank the International Institute of Noise Control Engineering for its support to attend the Inter-Noise 2016 Congress. In addition, many thanks go to Steffie de Groot for her assistance in this project.

REFERENCES

1. Attenborough K, Li KM, Horoshenkov K. Predicting outdoor sound. CRC Press; 2006.
2. Brandão E, Lenzi A, Paul S. A Review of the In Situ Impedance and Sound Absorption Measurement Techniques. Acta Acustica united with Acustica. 2015 May 1;101(3):443-63.
3. Nocke C, Mellert V, Waters-Fuller T, Attenborough K, Li KM. Impedance deduction from broad-band, point-source measurements at grazing incidence. Acta Acustica United with Acustica. 1997 Nov 1;83(6):1085-90.
4. Taherzadeh S, Attenborough K. Deduction of ground impedance from measurements of excess attenuation spectra. The Journal of the Acoustical Society of America. 1999 Mar 1;105(3):2039-42.
5. Dutilleux G, Vigran TE, Kristiansen UR. An in situ transfer function technique for the assessment of the acoustic absorption of materials in buildings. Applied Acoustics. 2001 May 31;62(5):555-72.
6. Van Renterghem T, Botteldooren D. In-situ measurements of sound propagating over extensive green roofs. Building and environment. 2011 Mar 31;46(3):729-38.
7. Connelly M, Hodgson M. Experimental investigation of the sound transmission of vegetated roofs. Applied Acoustics. 2013 Oct 31;74(10):1136-43.
8. Liu C, Hornikx M. Determination of the impedance of vegetated roofs with a double-layer Miki model. In Proceedings of Euronoise, 2015.
9. Hess HM, Attenborough K, Heap NW. Ground characterization by short‐range propagation measurements. The Journal of the Acoustical Society of America. 1990 May 1;87(5):1975-86.
10. NORDTEST A. 104: Ground Surfaces: Determination of Acoustic Impedance (1998). http://www.nordtest.info/index.php/methods/item/ground-surfaces-determination-of-the-acoustic-impedance-nt-acou-104.html (Last viewed 05/05/16).
11. Kuttruff H. Acoustics: An Introduction. CRC Press; 2007 Jan 24.
12. Kruse R, Mellert V. Effect and minimization of errors in in situ ground impedance measurements. Applied Acoustics. 2008 Oct 31;69(10):884-90.
13. Kruse R, Sauerzapf S. Reducing the influence of microphone errors on in-situ ground impedance measurements. Acta Acustica united with Acustica. 2009 Jan 1;95(1):151-5.
14. Attenborough K, Bashir I, Taherzadeh S. Outdoor ground impedance models. The Journal of the Acoustical Society of America. 2011 May 1;129(5):2806-19.